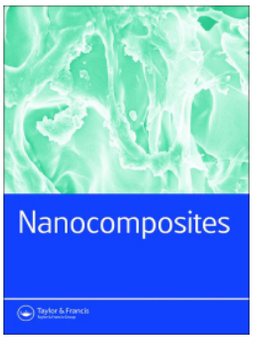

Nanocomposites

ISSN: (Print) (Online) Journal homepage: https://www.tandfonline.com/loi/ynan20

Crosslinked PAES-based sandwich-structured polymer nanocomposites with covalently strengthened interface towards high-temperature capacitive energy storage

Qiannan Cai, Danying Zhao, Hai Xu, Wenhan Xu, Hongyan Yao & Yunhe Zhang

To cite this article: Qiannan Cai, Danying Zhao, Hai Xu, Wenhan Xu, Hongyan Yao & Yunhe Zhang (2023) Crosslinked PAES-based sandwich-structured polymer nanocomposites with covalently strengthened interface towards high-temperature capacitive energy storage, Nanocomposites, 9:1, 10-17, DOI: 10.1080/20550324.2023.2173053

To link to this article: https://doi.org/10.1080/20550324.2023.2173053

NANOCOMPOSITES
2023, VOL. 9, NO. 1, 10–17
https://doi.org/10.1080/20550324.2023.2173053

Taylor & Francis
Taylor & Francis Group

RESEARCH ARTICLE

OPEN ACCESS Check for updates

Crosslinked PAES-based sandwich-structured polymer nanocomposites with covalently strengthened interface towards high-temperature capacitive energy storage

Qiannan Cai[a], Danying Zhao[a], Hai Xu[a], Wenhan Xu[b], Hongyan Yao[a] and Yunhe Zhang[a]

[a]College of Chemistry, Jilin University, Changchun, P. R. China; [b]Deutsches Elektronen-Synchrotron DESY, Hamburg, Germany

ABSTRACT

As a key material for capacitors, high-performance polymer dielectric films still exhibit the problem of low energy storage density, which cannot meet the requirements of high-power and high-temperature conditions. Here, a sandwich-structured composite film with inner layer doped TiO_2-BCB (titanium dioxide – benzocyclobutene) and outer layer doped BN-BCB (boron nitride – benzocyclobutene) nanoparticles was prepared, which exhibits reduced dielectric loss, leakage current and enhanced dielectric constant (ε) and breakdown strength (E_b). Diels-Alder reaction and radical polymerization reactions are utilized to form the entire cross-linked sandwich structure. Moreover, the thermal-induced crosslinked structure replaces the traditional multilayer structure established by Van der Waals forces, thus improving the dielectric and mechanical qualities of the film. Specifically, the sandwich structure composites achieved a large discharge energy density (4.0 J/cm^3) and high charge-discharge efficiency (84%) at 150 °C and 450 MV/m, and the dielectric dissipation factor is less than 0.005. These results demonstrated that designing a cross-linked network in multilayer nanocomposite structure is a feasible method to improve the high-temperature energy storage performance of these films.

GRAPHICAL ABSTRACT

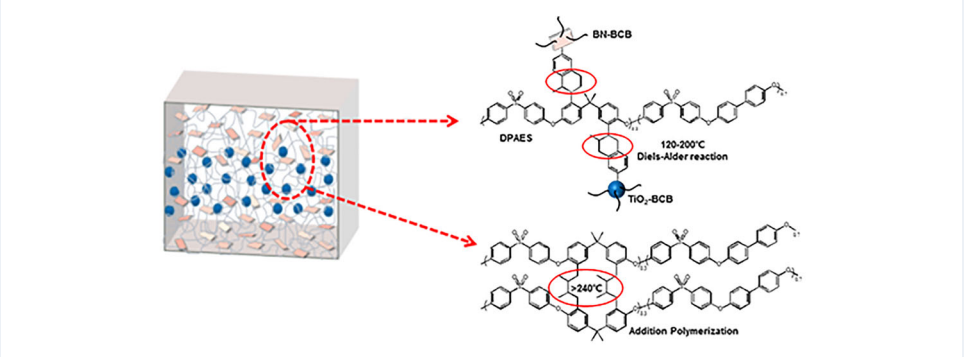

ARTICLE HISTORY
Received 10 June 2022
Accepted 27 November 2022

KEYWORDS
Dielectrics; nanocomposites; polyether sulfone; capacitive energy storage; sandwich structure; capacitors; polymer matrix; titanium dioxide

1. Introduction

With the development of pulsed power systems, power converters, new energy vehicles, and other fields that require high power density, dielectric film capacitors have been widely used owing to their rapid charge and discharge rate, excellent power density and long service life [1–3]. However, the core material such as capacitors, high-performance polymer dielectric films still pose the problem of low energy storage density. Generally, the dielectric dissipation factor is about 0.1–0.3 inneat polymer films. Modern power electronics require polymer film capacitors with low dielectric dissipation factor (lower than 0.003) which can operate at high temperatures (≥140 °C) for periods of time, in recent year a significant amount of work has been done to address this problem [4, 5].

Recently, nanocomposites became the focus of development due to their advantages of dielectric breakdown resistance and high dielectric constant (ε) of polymer and ceramic particles [6–9]. Among them, titanium dioxide (TiO_2) and boron nitride nanosheets (BN) are important inorganic fillers due to their excellent properties [10, 11]. The particle

CONTACT Hai Xu xuhai@jlu.edu.cn; Yunhe Zhang zhangyunhe@jlu.edu.cn College of Chemistry, Jilin University, Changchun 130012, P. R. China

Supplemental data for this article can be accessed online at https://doi.org/10.1080/20550324.2023.2173053.

diameter of anatase TiO_2 filler is less than 11 nm. The particle diameter of rutile TiO_2 filler is larger than 35 nm. In particular, the rutile crystalline possesses few internal defects, which is stable at high temperatures (1000 °C) [12]. Rutile TiO_2, as a semiconductor material, possessing a wide forbidden band-gap (3.5 eV) and a high ε (110) [13, 14]. The strong interactions between TiO_2 and some polymers are often used as a modifier or object of modification [7, 15, 16]. Although the ε of hexagonal BN is 4, they possess a wider forbidden band gap (5.97 eV) and higher thermal conductivity (300 W/mK) [17, 18]. The Advanced Power Electronics and Electric Motor Program at the Department of Energy proposed that film capacitors for electric vehicles should have high temperature tolerance (140 °C), long lifetime (>20,000 h), low loss ($\tan\delta < 0.005$), small volume (<0.6 L at 1 mF), and low cost (<$30/mF) [19]. However, the energy storage efficiency of the composites after doping with inorganic nanoparticles is still unable to meet requirements, which is due to the electric field distortion at the interface between the inorganic nanofillers and the polymer matrix. Electric field distortion is more likely to cause an increase in leakage current at high temperatures and thus a decrease in breakdown strength, becomes a non-negligible problem [20, 21]. To solve this problem, multilayer structured films have attracted the attention of researchers. On the one hand, the interfacial polarization between the layers facilitates the enhancement of the ε, which expands the local field state and facilitates the carrier trapping. On the other hand, multilayer structured films are rich in structural diversity [22]. Specifically, the ε of different layers are adjusted to optimize the electric field distribution, suppress the leakage current, and improve the breakdown strength (E_b) [23]. These advantages produce one of the most effective methods to enhance the energy storage performance of dielectric materials in high-temperature environments nowadays. Usually, multilayer polymer films are prepared by combining several layers of films by high pressing, hot compaction or solution casting layer by layer [24, 25]. Most preparation methods rely on non-covalent bonds, such as electrostatic attraction, hydrogen bonding, or other Van der Waals forces, which may result in large differences between the two phases and uneven texture due to insufficient bonding, introducing defects and thus limiting the effect of reducing leakage currents.

In this paper, a sandwich structured composite film was prepared by thermal cross-linking method based on layer upon layer doctor-blade coating starting from the optimization of the preparation process. The polymer matrix of all three layers is modified polyethersulfone, the outer layer is doped with BN-BCB, the middle layer is doped with TiO_2-BCB. This manner increases the density of the material, improves the local state and enhances the ability to limit the leakage current. Moreover, it increases the mechanical properties of the material and enhance the E_b and practicality of the film. BN is doped into the outer layers because it possesses a wider forbidden band gap and could block the injection of electrode charges. TiO_2 is doped into the inner layer because of high ε. The doping of modified nanofillers optimized the interfacial compatibility and dispersion of polymer matrix and filler particles, which improved the energy storage capacity of the composites in different aspects. The cross-linking system is derived from the self-crosslinking polycondensation reaction of polymer matrix and the cross-linking networks between the polymer and nanoparticles are formed by the Diels-Alder reaction.

2. Results and discussion

2.1. Material preparation and microstructure

Figure 1a shows a schematic diagram of the preparation of the three-layer film. This layer-by-layer doctor-blading method could shape the film in a short time, thereby avoiding problems such as settling of the composite material. The obtained multilayer nanocomposite film is dense, uniform, smooth and flexible (Figure 1b). As shown in Figure 1c, the cross-linked structure is composed of two reaction gradients, both within the monolayer and between the layers. the crosslinked structure is generated by two reactions, which occur within the monolayer and the interface of the interlayer. After the film is cured by layer-by-layer spin coating, at the temperature range of 120 °C to 200 °C, the BCB modified on the surface of the nanoparticle and the double bond on the polymer segment will crosslink through Diels-Alder reaction. When the temperature is exceeds 200 °C, the interlayer junctions of the polymers will be intertwined and penetrated, resulting in a compact and uniform structure. Then, when the temperature is higher than 240 °C, the polymer matrix relies on the double bond to undergo a self-crosslinking reaction, imprisoning the molecular segments, and the bonding between the interfaces changes from Van der Waals force to covalent bond, forming a cross-linked structure as shown in Figure 1d. The existence of these cross-linking methods optimizes the interface structure and reduces losses.

The field emission scanning electron microscope (FESEM) experiments were performed on the three-layer composite film, and the entire cross-section of the three-layer composite film can be clearly seen in

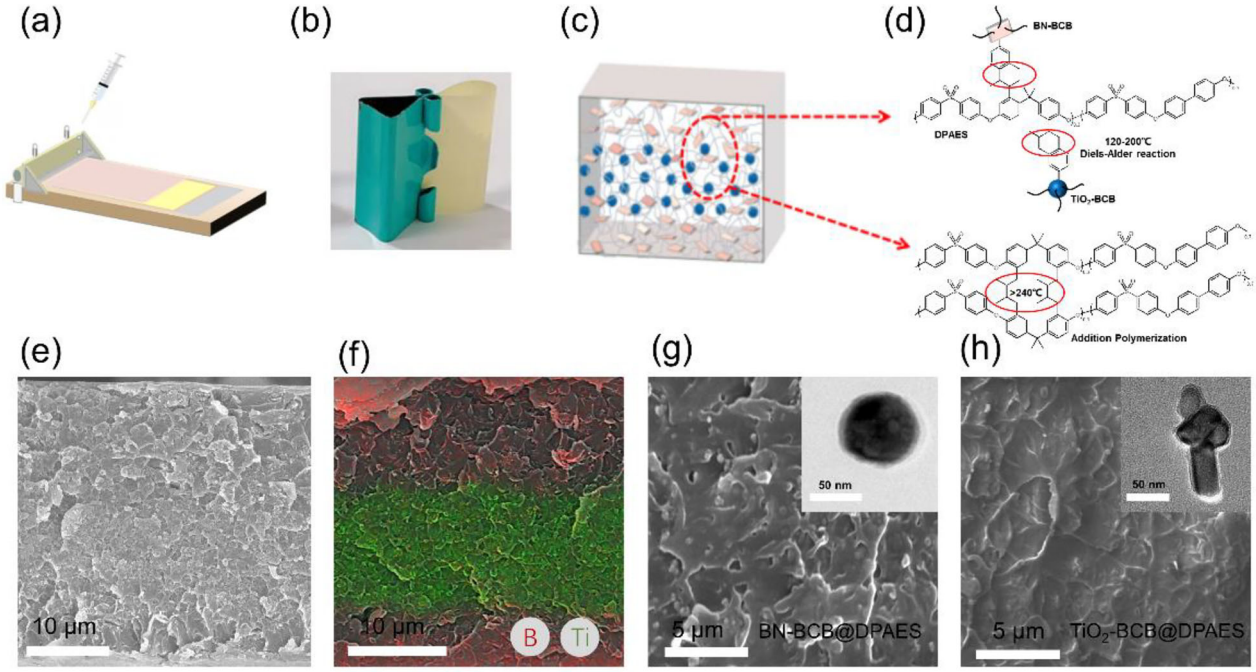

Figure 1. Preparation and morphology of 10 vol% BN-BCB/TiO_2-BCB/BN-BCB@DPAES. (a) Schematic diagram of the preparation process of the sandwich structured nanocomposite film. (b) Photographs of the bend sandwich structured nanocomposite film. (c) Schematic diagram of simple structural model of the sandwich structured nanocomposite film. (d) Schematic diagram of molecular structure and hot crosslinking methods. (e) Cross-sectional SEM image of the film. (f) EDS element distribution of the sandwich structured nanocomposite film. (Red stands for B element, green stands for Ti element.) (g) SEM image of 10 vol% BN-BCB@DPAES. (Inset is the TEM imagine of BN-BCB.) (h) SEM image of 10 vol% TiO_2-BCB@DPAES (Inset is the TEM imagine of TiO_2-BCB.).

Figure 1e. The overall structure is uniform, and the adjacent layers are closely combined. Different from the classic sandwich structure material, the three-layer structure composite material obtained by chemical cross-linking method in this work is relatively compact and uniform, which does not show the obvious delamination phenomenon of the traditional sandwich structure, and the boundary between the layers is not obvious [26]. However, a clear and uniform layered distribution can be clearly observed from the surface distribution map of the energy-dispersive X-ray spectroscopy (EDS) elements corresponding to the filler particles (Figure 1f). The Ti element is concentrated in the middle part of the multilayer film, and the B element is dispersed on both sides. The formation of this structure and morphology is achieved through interlayer cross-linking. In the classical layer-by-layer spin-coating process, the layer-to-layer bonding relies on the polymer solution dissolving the surface of the underlying film. However, under heat-solid conditions, the penetration time of this solvent is not long enough to smooth out the interface defects. The multilayer films prepared by conventional methods possess distinct interfaces and the polymer chain segments between the interfaces are formed by non-covalent bonds. Figures 1g and 2h show the homogeneity of the monolayer films after crosslinking. The filler content of nanoparticles is set at 10 vol% to provide optimal dielectric properties [27]. The modified nanoparticles are uniformly dispersed in the polymer matrix without causing agglomeration, so the dense structure at the interlayer interface can also be predicted. In general, the current approach aims to solve the interface problem of sandwich-structured films by transforming the Van der Waals forces of traditional interfaces into chemical crosslinking bonds, which enhances the uniformity at the interface, thereby enhancing its high-temperature energy storage performance. In general, this paper achieves the enhancement of the high-temperature energy storage performance of sandwich structured films by converting the non-covalent bonds at the conventional interfaces into chemical cross-linked bonds.

2.2. Dielectric properties

Figure 2a shows the comparison of the sandwich-structured nanocomposite film and single-layer nanocomposite films in the temperature dependence of the dielectric constant at 1 kHz. The dielectric constant of the single layer 10 vol% TiO_2-BCB@DPAES which is used as the intermediate layer is 7.2, the dielectric constant of 10 vol% BN-BCB@DPAES is 3.9, and the dielectric constant of the prepared 10 vol% BN-BCB/TiO_2-BCB/BN-BCB@DPAES is 6.1 at 100 °C. From 40 °C to

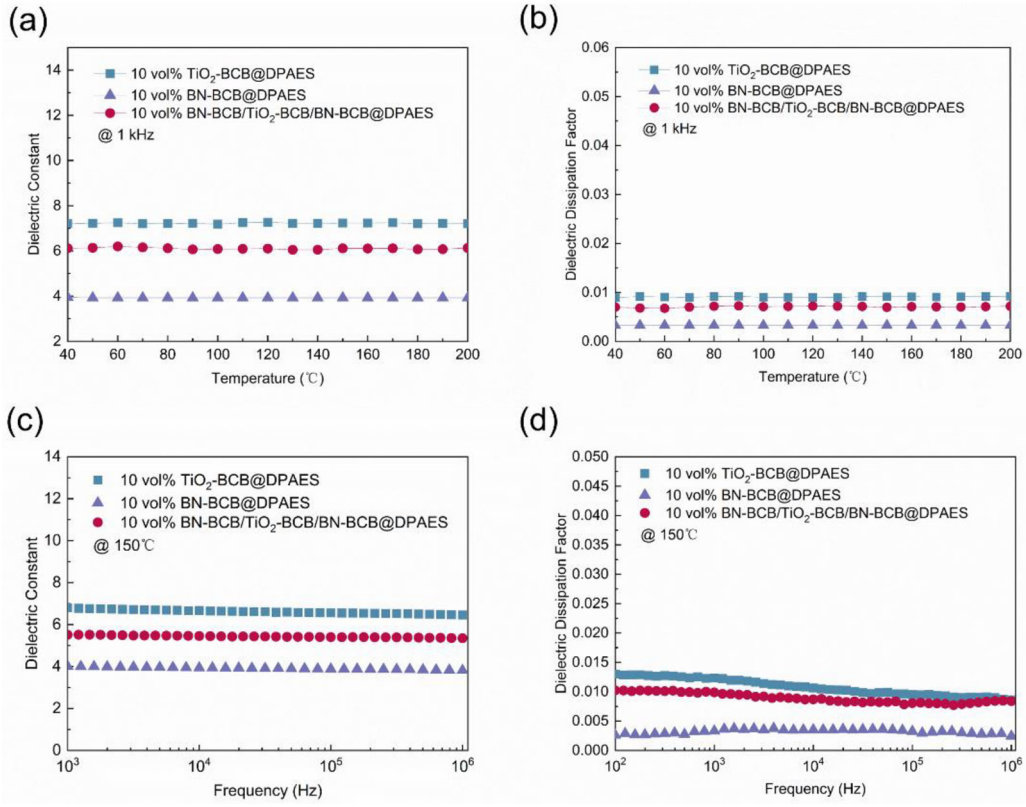

Figure 2. (a) Dielectric constant of single-layer nanocomposite films and sandwich structured nanocomposite film as a function of temperature at 1 kHz. (b) Dielectric dissipation factor of single-layer nanocomposite films and sandwich structured nanocomposite film as a function of temperature at 1 kHz. (c) Dielectric constant of single-layer nanocomposite films and sandwich structured nanocomposite film as a function of frequency at 150 °C. (d) Dielectric dissipation factor of single-layer nanocomposite films and sandwich structured nanocomposite film as a function of frequency at 150 °C.

200 °C, the dielectric constant of the sandwich-structured nanocomposite film is stable with a fluctuation of no more than 2%. Figure 2b shows the dielectric dissipation factor of single-layer nanocomposite films and sandwich structured nanocomposite film at a frequency of 1 kHz. The dielectric dissipation factor is the ratio of imaginary permittivity to real permittivity, which represents the loss of heat generated caused by the coupling of dielectric film and microwave. The dielectric dissipation factor of 10 vol% BN-BCB/TiO_2-BCB/BN-BCB@DPAES film is below 0.007 from 40 °C to 200 °C. According to Figure 2c, the estimation of the intrinsic dielectric constant, the dielectric constant of the sandwich structure film should be closer to the 10 vol% BN-BCB@DPAES monolayer with a large volume content. However, it is closer to 10 vol% TiO_2-BCB@DPAES which can be explained by the interface polarization, which has a negative effect on the dielectric constant. Moreover, as mentioned before, the interaction between the TiO_2 and the polymer matrix is comparatively strong. Due to its wide band gap, high mechanical strength (800 MV/m) [28], high thermal conductivity and low density (2.29 g/cm^{-3}, compared with other ceramic particles), BN can be used as an effective barrier to prevent leakage current and space charge conduction, resulting in improved breakdown strength and reduced conduction loss of dielectric composites. Thanks to the existence of the cross-linked structure, the movement of molecular segments is restricted in a certain area. In Figure 2d, the cross-linked interface structure reduces defects and reduces the dielectric dissipation factor by a certain extent. The stability of 10 vol% BN-BCB/TiO_2-BCB/BN-BCB@DPAES is reliable at different frequencies and temperatures. The permittivity and dielectric dissipation factor of 10 vol% BN-BCB/TiO_2-BCB/BN-BCB@DPAES is reliable at different frequencies and temperatures.

2.3. Energy storage performance

The E_b of the nanocomposite films at 150 °C are shown in Figure 3a which were analyzed by two-parameter Weibull distribution [29]. Specifically, the E_b of 10 vol% TiO_2-BCB@DPAES and 10 vol% BN-BCB@DPAES are 428 MV/m and 544 MV/m, respectively. And, while the E_b of the 10 vol% BN-BCB/TiO_2-BCB/BN-BCB@DPAES is 555 MV/m. Generally speaking, the breakdown strength of pure polymer films is between 300 MV/m and 700 MV/m. It can be found that the E_b of the cross-linked films possess appreciable strength comparing to recently

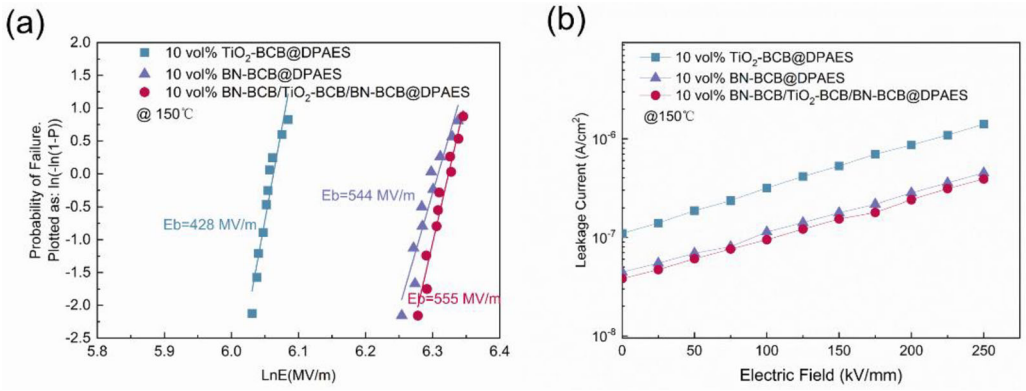

Figure 3. (a) Weibull distribution diagrams of single-layer nanocomposite films and sandwich structured nanocomposite film at 150 °C. (b) Leakage current density of single-layer nanocomposite films and sandwich structured nanocomposite film at 150 °C.

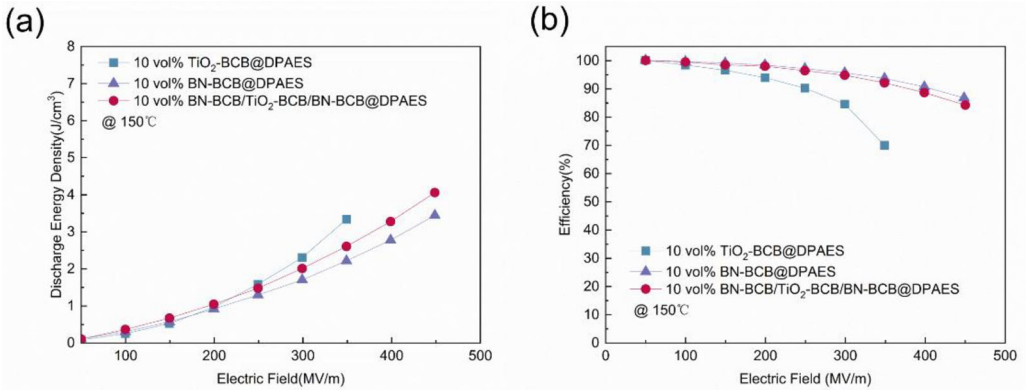

Figure 4. (a) Discharge energy density of single-layer nanocomposite films and sandwich structured nanocomposite film at 150 °C. (b) Charge and discharge efficiency of single-layer nanocomposite films and sandwich structured nanocomposite film at 150 °C.

reported multilayer-structured nanocomposites. The interlayer interface of sandwich structured film enriches the local state and increases the trapping energy level, therefore limiting the leakage current and improving the E_b [30]. Figure 3b shows the leakage current dependence of the electric field of nanocomposites at 150 °C. In general, the leakage currents are mainly due to the motion of charge carriers which are injected from the electrodes and accumulate inside the material prior to its breakdown. Figure 3b shows that the leakage current density of the sandwich structured nanocomposite film is lower than that of the single layer nanocomposite films at 150 °C. It indicates that the cross-linking network between the two modified core-shell nanoparticles and the polymer matrix, and the cross-linking structure of the interlayer interface can reduce the charge transport in the sandwich structure nanocomposites. Furthermore, the charge transport originates from the filler between matrix and the layer-to-layer. Thus, the conduction loss and leakage current are reduced, and E_b is increased. Moreover, the distance between polymer chains decreases in the crosslinked structure due to a more regular arrangement, thus compacting the film. Crosslinked structure increases the mechanical strength (Tensile stress-strain curves in Supporting Information Figure S3) of polymer films and reduces the possibility of electromechanical breakdown.

Figure 4a shows the discharge energy density of sandwich structure nanocomposite and corresponding monolayer films at 150 °C. For linear dielectrics [31], the energy storage density can be calculated by:

$$U_e = \frac{1}{2}\varepsilon_0\varepsilon_r E_b^2 \quad (1)$$

ε_o is the vacuum dielectric constant, ε_r is the relative dielectric constant of the dielectric materials. It can be inferred from the formula that U_e is proportional to its ε, so the introduction of TiO_2 with high ε in sandwich structured nanocomposite film can significantly increase the U_e. The discharge energy density of sandwich structured nanocomposite film is higher than that of any other two single layer nanocomposite films, reaching 4 J/cm^3 at 450 MV/m, which is attributed to its high ε and low dissipation factor. Generally, the charge-discharge efficiency of multilayer nanocomposites is affected by the interface properties. The interface between the filler nanoparticles and the matrix has a

significant impact on the charge transfer, leakage current and the breakdown strength. Figure 4b shows the charge and discharge efficiency is improved by constructing an interconnection network in the sandwich structured nanocomposite film. At 150 °C, the charge-discharge efficiency of 10 vol% BN-BCB/TiO_2-BCB/BN-BCB@DPAES reaches more than 84% at 450 MV/m. The above results demonstrated that the sandwich structure with cross-linked network effectively improve the energy storage performance at high temperature.

3. Conclusion

The interlayer structure of sandwich structured nanocomposite film is optimized by crosslinking. The multilayer structured polymer-based dielectric nanocomposite film is whole crosslinking derived from Diels-Alder reaction and radical polymerization. Interlayer interactions in the resulting films change from non-covalent bonds to more stable chemical covalent bonds, which endows the nanocomposite film denser and reduces internal defects between layers, making the film more complete and uniform. The dielectric properties of the sandwich structured nanocomposite and two single-layer nanocomposite are systematically compared. Among them, the sandwich structured nanocomposite film exhibits excellent dielectric stability and a low dissipation factor at 150 °C, indicating that the crosslinked network established by doping TiO_2 in the inner layer can effectively limit the movement of polymer chain segments at 150 °C. Specifically, the discharge energy density of 10 vol% BN-BCB/TiO_2-BCB/BN-BCB@DPAES reaches 4.0 J/cm^3 (450 MV/m) at 150 °C with a charge-discharge efficiency of 84%. The sandwich structured nanocomposite film combines the both advantages of two types of single-layer films. It provides an effective approach for optimizing sandwich structured composite films and possesses broad application prospects in the field of dielectric energy storage at high temperature.

4. Experimental section

4.1. Materials

The boron nitride (100 nm), titanium dioxide (100 nm) and palladium acetate (II) used in the experiment were purchased from Shanghai Aladdin Biochemical Technology Co., Ltd. An aqueous solution of H_2O_2 (30 wt%) and 3-(trimethoxysilyl) propyl methacrylate (MPS) was used as the coupling agent. Tris(o-tolyl) phosphine (98%) was purchased from Johnson, 4-Bromobenzocyclobutene (4-Br-BCB, 97%) was purchased from Chem-target Technologies Co., Ltd., N,N-dimethylformamide (DMF, 99.9%) first passed standard procedures dry and distilled fresh before use. N,N-Dimethylacetamide (DMAc, 99.9%), K_2CO_3 and toluene are all used without further purification. The synthesis of DPAES was performed according to previously reported procedures [28].

4.2. Synthesis and characterization of benzocyclobutene surface functionalized TiO_2 and BN

The same method was used to obtain functionalized TiO_2 and BN nanoparticles: First, after adding 15 g of nanoparticles to 300 mL of 30 wt% hydrogen peroxide aqueous solution, ultrasonic treatment for 30 min, and then reflux in an oil bath at 100 °C for 4 h. Finally, centrifugation is performed to obtain nanoparticles (9000 r min^{-1}, 5 min), which are vacuum dried at 80 °C for 12 h to obtain hydroxylated nanoparticles. Secondly, 5 g of hydroxylated nanoparticles were added to a three-necked flask containing 80 mL, KH570 was added after ultrasonic dispersion, the mixture was heated to 80 °C for 24 h under N_2 atmosphere, and the nanoparticles were recovered by centrifugation at 9000 rpm for 5 min. The obtained nanoparticles were vacuum dried at 80 °C for 12 h. Finally, under the conditions of argon, 3.125 g of particles were added to the DMF solution containing 80 mL. After ultrasonic dispersion, 0.3 g 4-Br-BCB, 0.007 g $Pd(OAc)_2$, 0.009 g P(o-tol)$_3$ and 0.076 g K_2CO_3, the mixture was heated to 80 °C and stirred for 24 h under argon conditions. After the reaction was completed, the nanoparticles were recovered by centrifugation and extracted with acetone for 12 h, and then vacuum dried at 80 °C for 12 h, named TiO_2-BCB and BN-BCB [26].

4.3. Preparation of multilayer nanocomposites

The modified BN-BCB (0.167 g, 2.25 g cm^{-3}) and TiO_2-BCB (0.448 g, 6.01 g cm^{-3}) nanoparticles were added to the DMAc (5 mL) solvent for ultrasonic dispersion. At the same time, the polyaryl ether sulfone containing pendant propylene groups (0.9 g, 1.34 g cm^{-3}) was dissolved in the DMAc and stirred for two hours. The particle solution was poured into the polymer solution and stirred again for 2 h. Using a film-scraping process and a glass plate as the substrate, the first layer and of polymer composite material filled with BN-BCB nanosheets was deposited, and after a simple heat treatment, the second layer of material filled with TiO_2-BCB nanoparticles was deposited. The third layer of film material is prepared in the same way as the first step. The multilayer composite film was heat-treated

at 240 °C for 2 h, then it was immersed in deionized water. The film thickness was about 15 μm, which is recorded as 10 vol% BN-BCB/TiO_2-BCB/BN-BCB@DPAES. Similarly, two single-layer composite films of the same thickness were prepared and recorded as 10 vol% BN-BCB@DPAES and 10 vol% TiO_2-BCB@DPAES films. The film thickness was controlled by the solution concentration and the doctor-blade deposition process.

Disclosure statement

The authors declare that they have no known competing financial interests or personal relationships that could have appeared to influence the work reported in this paper.

Funding

This work was financially supported by the National Natural Science Foundation of China (Nos. 51973080, 92066104, 52003099).

Notes on contributors

Qiannan Cai is graduated student in the college of chemistry of Jilin University. She has worked on composites multilayer film.

Danying Zhao is a doctoral researcher in the College of chemistry of Jilin University. She has worked on dielectric and energy storage properties of polymer films applications.

Hai Xu received Doctor of Science degree and affiliation is College of Chemistry, Jilin University. Research interests are synthesis, molecular simulation and quantum chemistry calculation of organic photoelectric functional materials.

Wenhan Xu is a postdoctoral researcher at the Deutsches Elektronen-Synchrotron DESY, Notkestr, Hamburg, Germany. He has published mainly on dielectric polymers applications.

Hongyan Yao received his Ph.D. degree from National University of Singapore in 2018 and is an associate professor in the College of chemistry of Jilin University. His current research interests are mainly focused on polymer electrode materials for lithium-ion batteries, polyimide porous materials, and fluorinated polyimide transparent low dielectric materials.

Yunhe Zhang is a professor of the College of chemistry of Jilin University. He is mainly engaged in the development and application technology research of special engineering plastics and coatings, and has published more than 100 academic papers in different journals.

ORCID

Yunhe Zhang http://orcid.org/0000-0001-8582-3353

References

1. Kum-Onsa P, Chanlek N, Thongbai P. Largely enhanced dielectric properties of TiO_2-nanorods/poly(vinylidene fluoride) nanocomposites driven by enhanced interfacial areas. Nanocomposites. 2021;7(1):123–131.
2. Gong L, Chen S-H, Zhan S-P, et al. An enhancement on the dielectric performance of poly(vinylidene fluoride)-based composite with graphene oxide-$BaTiO_3$ hybrid. Nanocomposites. 2019;5(2):61–66.
3. Tang Y, Xu W, Niu S, et al. Crosslinked dielectric materials for high-temperature capacitive energy storage. J Mater Chem A. 2021;9(16):10000–10011.
4. Li Q, Chen L, Gadinski MR, et al. Flexible high-temperature dielectric materials from polymer nanocomposites. Nature. 2015;523(7562):576–579.
5. Li Q, Yao F-Z, Liu Y, et al. High-temperature dielectric materials for electrical energy storage. Annu Rev Mater Res. 2018;48(1):219–243.
6. Tanaka T. Dielectric nanocomposites with insulating properties. IEEE Trans Dielect Electr Insul. 2005;12(5):914–928.
7. Thakur VK, Gupta, RK, Prateek. Recent progress on ferroelectric polymer-based nanocomposites for high energy density capacitors: synthesis, dielectric properties, and future aspects. Chem Rev. 2016;116(7):4260–4317.
8. Wang T, Peng R-C, Peng W, et al. 2-2 Type PVDF-based composites interlayered by epitaxial (111)-oriented BTO films for high energy storage density. Adv Funct Mater. 2022;32(10):2108496.
9. Luo B, Wang X, Tian E, et al. Interfacial electronic properties of ferroelectric nanocomposites for energy storage application. Mater Today Energy. 2019;12:136–145.
10. Zha J-W, Song H-T, Dang Z-M, et al. Mechanism analysis of improved corona-resistant characteristic in polyimide/TiO_2 nanohybrid films. Appl Phys Lett. 2008;93(19):192911.
11. Mansor NS, Hamzah MS, Kamarol M, et al. A comparative study of dielectric strength between SiR/EPDM and PP/EPDM blends with various type of nanofillers. AMR. 2013;832:483–487.
12. Zha J-W, Dang Z-M, Zhou T, et al. Electrical properties of TiO_2-filled polyimide nanocomposite films prepared via an in situ polymerization process. Synth Met. 2010;160(23-24):2670–2674.
13. Liang F, Zhang L, Lu W-Z, et al. Dielectric performance of polymer-based composites containing core-shell Ag@TiO_2 nanoparticle fillers. Appl Phys Lett. 2016;108(7):072902.
14. Aaditya VB, Bharathesh BM, Harshitha R, et al. Study of dielectric properties of polypyrrole/titanium dioxide and polypyrrole/titanium dioxide-MWCNT nano composites. J Mater Sci Mater Electron. 2018;29(4):2848–2859.
15. Xiong X, Zhou Z, Zhang Z, et al. Facile preparation and enhanced dielectric performance of rod-like TiO_2/P(VDF-TrFE-CFE) composites. J Mater Sci Mater Electron. 2018;29(16):14161–14169.
16. Kang D, Wang G, Huang Y, et al. Decorating TiO_2 nanowires with $BaTiO_3$ nanoparticles: a new approach leading to substantially enhanced energy storage capability of high-k polymer

nanocomposites. ACS Appl Mater Interfaces. 2018; 10(4):4077–4085.
17. Zhu Y, Zhu Y, Huang X, et al. High energy density polymer dielectrics interlayered by assembled boron nitride nanosheets. Adv Energy Mater. 2019;9(36): 1901826.
18. Shen Y, Zhang X, Li M, et al. Polymer nanocomposite dielectrics for electrical energy storage. Natl Sci Rev. 2017;4(1):23–25.
19. Ju T, Chen X, Langhe D, et al. Enhancing breakdown strength and lifetime of multilayer dielectric films by using high temperature polycarbonate skin layers. Energy Storage Mater. 2022;45:494–503.
20. Li Y, Zhou Y, Zhu Y, et al. Polymer nanocomposites with high energy density and improved charge-discharge efficiency utilizing hierarchically-structured nanofillers. J Mater Chem A. 2020;8(14): 6576–6585.
21. Nan CW, Shen Y, Ma J. Physical properties of composites near percolation. Annu Rev Mater Res. 2010;40(1):131–151.
22. Uyor UO, Popoola API, Popoola OM, et al. Thermal, mechanical and dielectric properties of functionalized sandwich BN-$BaTiO_3$-BN/polypropylene nanocomposites. J Alloys Compd. 2022;894:162405.
23. Pei J-Y, Zha J-W, Zhou W-Y, et al. Enhancement of breakdown strength of multilayer polymer film through electric field redistribution and defect modification. Appl Phys Lett. 2019;114(10):103702.
24. Wang Z, Fan J, Guo X, et al. Enhanced permittivity of negative permittivity middle-layer sandwich polymer matrix composites through conductive filling with flake MAX phase ceramics. RSC Adv. 2020;10(45):27025–27032.
25. Lin Y, Sun C, Zhan S, et al. Two-dimensional sheet-like $K_{0.5}Na_{0.5}NbO_3$ platelets and sandwich structure induced ultrahigh discharge efficiency in poly (vinylidenefluoride)-based composites, compos. Sci Technol. 2020;199:108368.
26. Ru J, Min D, Lanagan M, et al. Enhanced energy storage properties of thermostable sandwich-structured $BaTiO_3$/polyimide nanocomposites with better controlled interfaces. Mater Des. 2021;197:109270.
27. Xu W, Liu J, Chen T, et al. Bioinspired polymer nanocomposites exhibit giant energy density and high efficiency at high temperature. Small. 2019; 15(28):1901582.
28. Wu HH, Zhuo F, Qiao H, et al. Polymer-/ceramic-based dielectric composites for energy storage and conversion. Energy Environ Mater. 2022;5(2):486–514.
29. Dean CR, Young AF, Meric I, et al. Boron nitride substrates for high-quality graphene electronics. Nat Nanotechnol. 2010;5(10):722–726.
30. Zhu T, Qian C, Zheng W, et al. Modified halloysite nanotube filled polyimide composites for film capacitors: high dielectric constant, low dielectric loss and excellent heat resistance. RSC Adv. 2018; 8(19):10522–10531.
31. Shen Y, Lin Y, Zhang QM. Polymer nanocomposites with high energy storage densities. MRS Bull. 2015;40(9):753–759.